

# The Future of Imaging in Pulmonary Hypertension: Better Assessment of Structure, Function, and Flow

Akhil Narang, MD  
Division of Cardiology, Department of  
Medicine  
Feinberg Cardiovascular Research Institute  
Northwestern University Feinberg School  
of Medicine  
Chicago, IL

Benjamin H. Freed, MD  
Division of Cardiology, Department of  
Medicine  
Feinberg Cardiovascular Research Institute  
Northwestern University Feinberg School  
of Medicine  
Chicago, IL

Cardiovascular imaging is essential in the evaluation and management of patients with pulmonary hypertension. Echocardiography and magnetic resonance imaging, in particular, provide basic measurements of pulmonary pressure and right ventricular function, but current technology allows for a much more comprehensive assessment. Many of these advancements have the potential to enhance risk stratification and provide additional phenotypic data that may strengthen or alter the therapeutic approach. This review will highlight multiple novel techniques from various imaging modalities and how this information can be applied in clinical practice.

## INTRODUCTION

The standard imaging evaluation of patients with known or presumed pulmonary hypertension (PH) includes the measurement of pulmonary arterial systolic pressure and the assessment of right ventricular (RV) size and function. While this information is certainly critical for the management of these patients, it is the very minimum of what current imaging technology can provide. Today, imaging modalities such as echocardiography and magnetic resonance imaging (MRI) can probe the pulmonary vasculature and deconstruct RV movement in new and exciting ways, providing greater mechanistic insight into the pathophysiology of this disease and a better understanding of how current therapies work. This review will focus on novel imaging techniques in PH, which have the potential to fundamentally change how we care for these patients.

## ECHOCARDIOGRAPHY

Mortality and morbidity of patients with PH is closely linked to the function and size of the RV. Accordingly, echocardiographic evaluation of patients

with known or suspected PH centers on attempts to accurately understand the RV. The anterior location of the RV within the thorax coupled with its complex geometry make echocardiographic assessment particularly challenging. No single echocardiographic view adequately captures the entirety of the chamber, either anatomically or with respect to functional analysis. Moreover, the complicated contraction of the RV (longitudinal fiber shortening along the lateral tricuspid annulus towards the apex, free wall inward movement or “bellows effect,” and anteroposterior free wall shortening over the shared ventricular septum) have resulted in the development of multiple quantitative parameters.<sup>1,2</sup>

### General Echocardiographic Analysis

Conventional echocardiographic assessment of RV size and function incorporates a number of 1- and 2-dimensional (2D) indices.<sup>3</sup> Size of the RV is often assessed using linear dimensions of the RV from a number of views including parasternal and apical views. RV function is often qualitatively evaluated,

though this is subject to considerable inter- and intra-observer variability. Quantitative assessment of RV function can be accomplished through several different techniques, most commonly: tricuspid annular plane systolic excursion (TAPSE), S' velocity, and fractional area change (FAC).

TAPSE (M-mode) reflects the basal to apical shortening or distance traveled of the lateral tricuspid valve annulus between end-diastole and end-systole while S' (tissue Doppler imaging) measures the myocardial systolic excursion velocity at lateral tricuspid annulus. Both TAPSE and S' primarily evaluate the longitudinal motion of the RV free wall while not incorporating the other aspects of RV contraction. Both of these parameters are also angle dependent and do not fully account for global RV function. RV FAC better reflects global RV function and relies upon accurate tracing of the RV end-diastolic area (EDA) and end-systolic area (ESA) where  $FAC = (EDA - ESA)/EDA$ .

Furthermore, beyond evaluation of RV systolic pressure and pulmonary artery (PA) pressures using Doppler echocardiography (through assessment of the RV-right atrial gradient or pulmonary regurgitation signal and modified Bernoulli equation), a complete noninvasive hemodynamic assessment is possible

Key Words—pulmonary hypertension, right ventricle, echocardiography, MRI, pulmonary vasculature  
Correspondence: benjamin.freed@northwestern.edu  
Disclosure: The authors have no relevant personal financial relationships to disclose.

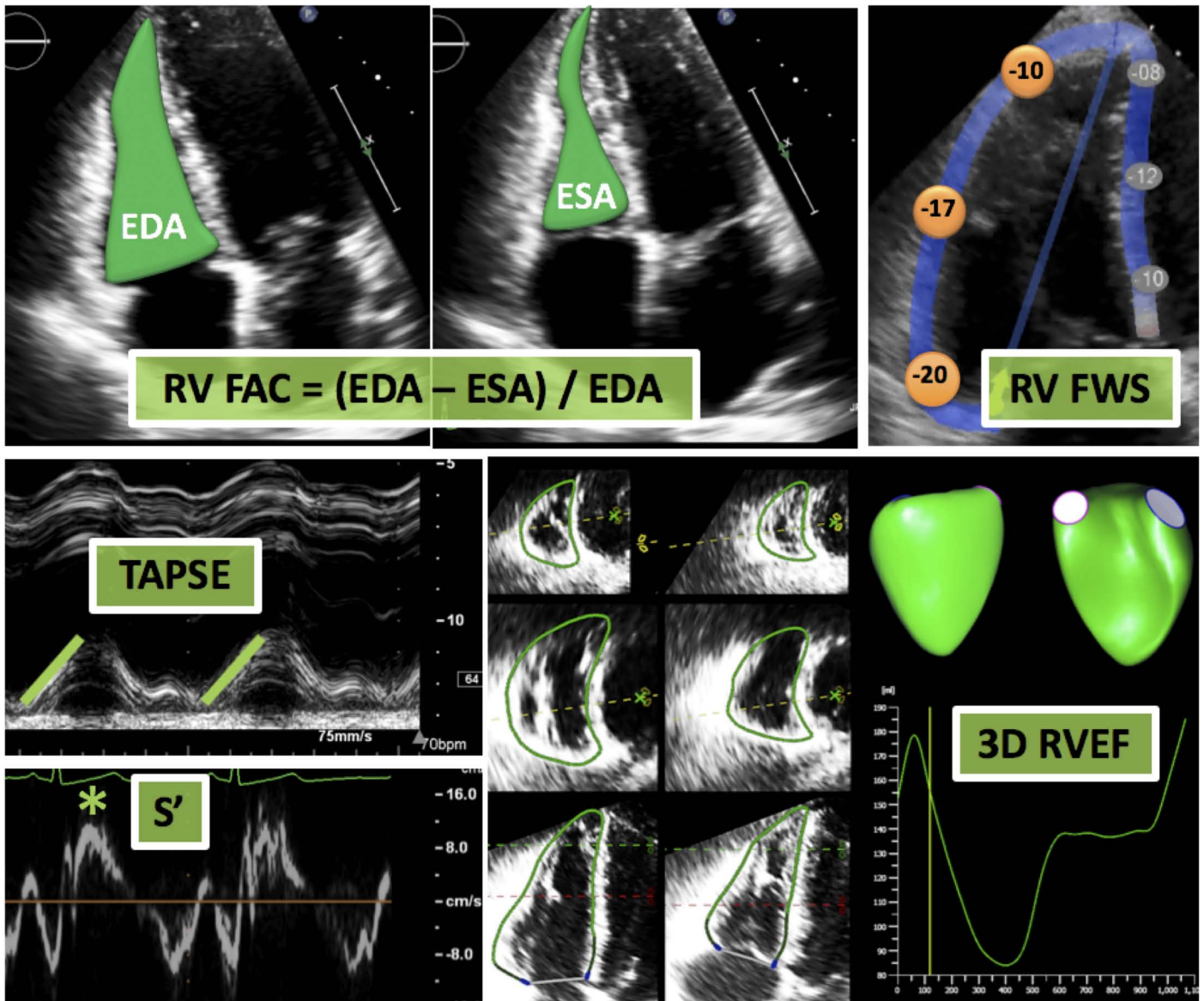


**Figure 1:** Echocardiographic assessment of RV function. RV = right ventricle; FAC = fractional area change; EDA = end-diastolic area; ESA = end-systolic area; FWS = free wall strain; TAPSE = tricuspid annular plane systolic excursion; 3D = 3-dimensional; RVEF = right ventricular ejection fraction.

and should routinely be performed. These parameters include right atrial pressure, pulmonary vascular resistance, and evaluation of left-sided pressures. Furthermore, other echocardiographic parameters such as a reduced PA acceleration time (pulsed-wave Doppler) and notching of the right ventricular outflow tract Doppler tracing are markers of significant PH.<sup>4</sup>

While these conventional echocardiographic RV parameters are helpful in understanding downstream consequences of PH on the size and function of the RV, each have their shortcomings. In recent times, there is emerging data

on the use of novel echocardiographic indices that, when coupled with conventional assessment, further enable the clinician to interrogate the sequelae of PH (Figure 1).

#### *Three-Dimensional (3D) Echocardiography*

The development and refinement of 3D echocardiography over the past several decades have allowed for tremendous progress in our understanding of the RV.<sup>5,6</sup> Through the transthoracic acquisition of a pyramid of ultrasound data, there is now the capability to obtain accurate volumetric measurements of the

RV, which much more closely reflect the “gold standard” of MRI.

Previous studies have confirmed 3D RV volumes measured by echocardiography better correlate with MRI measured volumes than 2D RV echocardiography volumes.<sup>7-9</sup> Accordingly, the calculation of 3D RV ejection fraction (EF) derived from 3D volumes represents another important index to evaluate RV size and function. 3D RVEF is the only parameter that fully incorporates global RV function throughout the cardiac cycle. Serial interrogation of 3D RV volumes and EF in response to therapies for PH (including diuretics) may yield import-

ant data that reflect RV remodeling over time. Adequate interpretation and analysis of 3D volume acquisitions of the RV depends on user experience and training and is often a barrier to widespread adaptation. The advent of artificial intelligence and machine learning may allow for greater incorporation of 3D echocardiography. Once 3D images are acquired, automated postprocessing analysis generates RV volumes and EF that are comparable to MRI assessment.<sup>10</sup>

### *RV Shape*

Remodeling of the RV in PH is also best understood using 3D echocardiography. 3D RV full-volume acquisitions can be segmented into endocardial surfaces from which RV shape can be determined. Parameters from these surface maps, namely curvature, are then quantifiable. In patients with PH, the RV septum is convex in curvature and bulges toward the left ventricle throughout the cardiac cycle unlike in normal subjects. Additionally, in PH (unlike healthy controls), the RV free wall and apex demonstrate convexity throughout the cardiac cycle.<sup>11–13</sup> Temporal changes in these differential, regional curvature changes during the course of therapy may be a useful means of monitoring disease progression or regression.

### *Tricuspid Regurgitation*

In patients with progressive PH, functional tricuspid regurgitation often results as a consequence of RV and tricuspid annular remodeling. The progression of tricuspid regurgitation in PH has been shown to be associated with progressive increasing all-cause mortality. From an echocardiographic standpoint, progressive tricuspid regurgitation has been associated with higher PA pressures, increasing RV enlargement, worsening RV sphericity, tricuspid annular dilation, and increasing tricuspid valve tenting area. Patients who experience worsening tricuspid regurgitation in serial imaging warrant special attention as this may suggest worse outcomes.<sup>14</sup>

### *RV Strain*

Myocardial deformation analysis is the underlying principle of strain. Speck-

le-tracking echocardiography (STE) is the predominant method by which strain is calculated. STE relies on tracking motion of ultrasound speckles throughout the cardiac cycle. The speckles are created as a result of ultrasound beam scatter and can be identified frame by frame as they move across systole and diastole. Tracking these speckles allows for the creation of strain and strain rate curves. STE relies on imaging at high frame rates, typically >50 frames/second. There are a number of benefits of strain imaging, namely that measurements generally reflect global function (accounting for abnormalities that occur throughout the cardiac cycle), and strain is angle- and mostly load-independent.<sup>15</sup>

Unlike the left ventricle, where longitudinal, circumferential, and radial strain are all useful parameters of myocardial deformation, the longitudinal strain of the RV best reflects the underlying myocardial fiber architecture of the RV. Furthermore, due to the shared septum between the right and left ventricles, the septal contribution to RV strain is typically ignored in favor of using the longitudinal strain of the RV free wall.

In patients with seemingly normal parameters of RV function, abnormalities in RV free wall longitudinal strain often reflect subclinical RV dysfunction before it may be readily apparent or measured by 1 or 2D echocardiographic parameters. Similarly, the RV free wall can be subdivided into the basal, mid, and apical segments. Regional RV remodeling in PH, in addition to other pathologies, can also be detected by regional strain changes.

In PH, abnormal RV free wall strain has been associated with worse outcomes and New York Heart Association functional class. The cutoff values for RV strain in PH vary from study to study, but improvements in strain are generally observed in response to medical therapy.<sup>16–18</sup> Worsening RV strain despite medical therapy should be seen as a sign of possible RV failure.

### *Impact on the Left Ventricle*

While PH is primarily thought of as a disease of the right heart, its impact on the left ventricle has recently become clearer. Generally the left ventricular

(LV) EF is preserved in PH, so when significant reduction in LVEF occurs, the prognosis is often dismal. However, when the LVEF is normal, newer work has shown LV global longitudinal strain is independently associated with death in addition to right-sided heart abnormalities.<sup>19</sup> In addition to routine assessment of RV strain, consideration should be given to following LV strain as well.

### **MRI**

The role for MRI in the evaluation of patients with PH is rapidly evolving. MRI is already considered the “gold standard” for assessment of RV volume, mass, and EF, and the prognostic utility of all of these measures in PH is well established.<sup>20</sup> In addition, MRI measurements of the pulmonary vasculature, including PA velocity, flow, and stiffness, have provided insights into the pathophysiology of PH and all show promise in the clinical workup of patients with this disease.<sup>20</sup> This review will highlight newer MRI techniques such as RV strain imaging, RV T1 mapping, and 4-dimensional (4D) flow of the pulmonary vasculature that move beyond standard cine and 2D phase contrast imaging. The use of exercise MRI and deep learning will also be discussed.

### *RV Strain Imaging*

As mentioned earlier, strain imaging measures myocardial deformation and is potentially a more sensitive metric of cardiac function than EF. RV strain is a strong predictor of outcomes in PH and adds incremental prognostic value to PA systolic pressure and other clinical variables.<sup>16,21,22</sup> Given its ability to provide volumetric coverage of the whole heart, MRI is uniquely positioned to evaluate RV strain in a number of cardiac conditions including PH.

One of the first publications to evaluate RV strain in PH showed reduced longitudinal strain in several RV segments despite normal RVEF, highlighting the superior sensitivity of RV strain to detect regional changes in function.<sup>23</sup> This study used strain encoded imaging which requires dedicated image acquisitions.

More recently, feature-tracking strain, which can be performed retro-

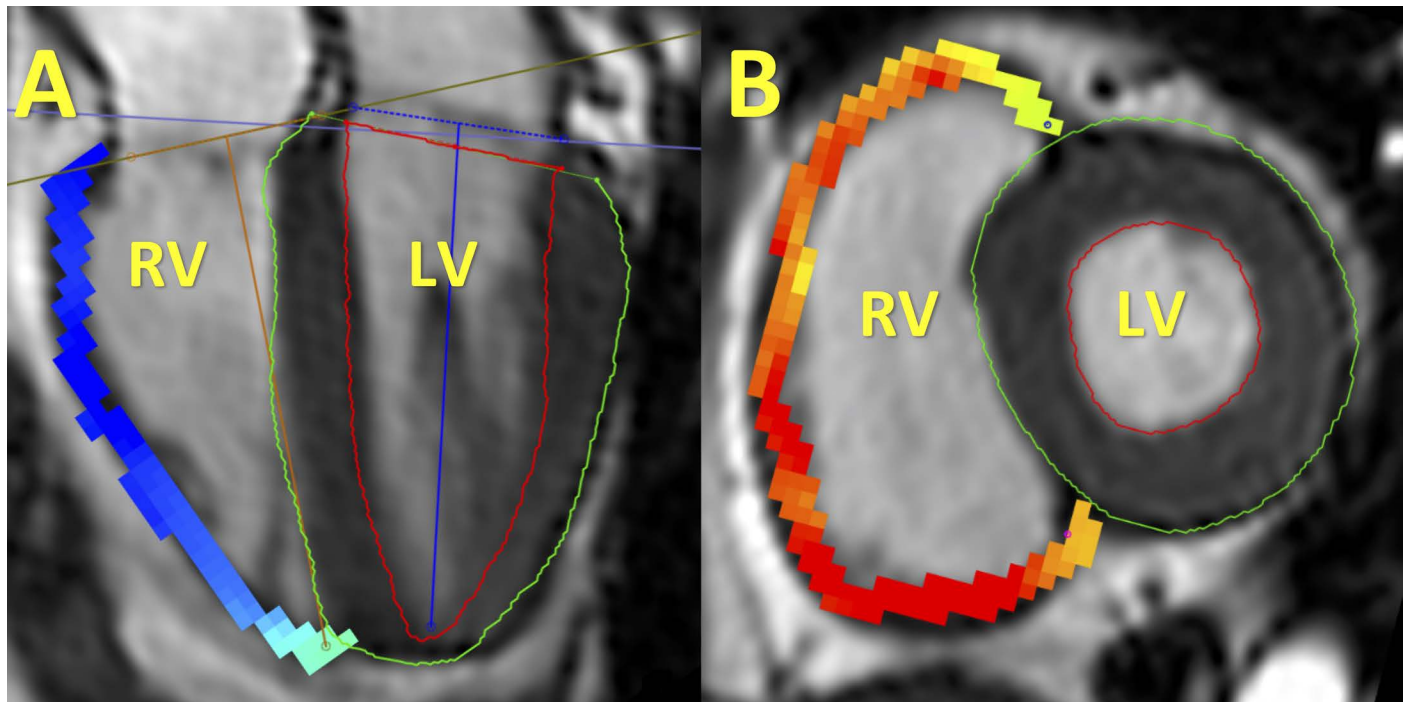


**Figure 2:** Feature tracking strain of the LV and RV. **(A)** RV and LV longitudinal strain analysis obtained from a four-chamber view. **(B)** RV and LV radial strain analysis obtained from a short-axis view. Strain analysis was performed on the software cvi42 by Circle Cardiovascular Imaging Inc, release 5.3.0 (364). RV = right ventricle; LV = left ventricle.

spectively using standard cine images, has shown promise in measuring RV strain (Figure 2, see also Supplemental Clips 1 and 2). In a study evaluating over 100 patients referred to MRI for PH evaluation, feature-tracking RV strain was feasible in 95% of patients and showed significantly reduced global circumferential strain rate in patients with normal RVEF.<sup>24</sup> Furthermore, RV strain was independently associated with the composite endpoint of death, lung transplantation, or functional class deterioration.

Tello et al. used pressure-volume loop measurements to help determine which RV indices are most associated with strain. In a study of 38 patients with PH who underwent conductance catheterization within 24 hours of feature-tracking RV strain, long-axis RV radial strain was associated with RV-PA coupling while RV longitudinal strain showed a significant association with RV end-diastolic stiffness.<sup>25</sup>

### RV T1 Mapping

One of the most unique capabilities of MRI is characterizing tissue abnormalities using gadolinium contrast. In PH, late gadolinium enhancement is

frequently detected in the RV insertion points, likely due to RV remodeling.<sup>26</sup> While commonly observed in this patient population, RV insertion point enhancement is rather nonspecific and is not independently associated with poor outcomes.<sup>27,28</sup> Recent work has focused on RV T1 mapping, a technique that allows for quantitative measurement of diffuse interstitial fibrosis in the RV. Several PH studies show a significant association between RV insertion point T1 time (a measure of myocardial fibrosis) and LV eccentricity or interventricular septal angle, measures of RV remodeling.<sup>29,30</sup> Similar to previous papers evaluating RV insertion point late gadolinium enhancement, Saunders et al. found no relationship between RV insertion point T1 time and outcomes.

Kawel-Boehm et al. examined T1 mapping of the RV free wall using standard modified look-locker inversion (an MRI sequence used for detecting myocardial fibrosis; MOLLI) recovery in 20 healthy controls.<sup>31</sup> The authors found that the average T1 time of the RV free wall was significantly longer than the left ventricle. The authors believed this was due to the naturally higher collagen content in the RV, but volume averaging

is also suspected. RV free wall T1 mapping was also evaluated in a recent study examining invasive pressure-volume loop measures in 42 patients with PH.<sup>32</sup> The authors found that RV free wall T1 time (when averaged with RV insertion point and interventricular septum T1 times) correlated significantly with end-diastolic stiffness but not RV-PA coupling.

Higher resolution T1 mapping sequences, which may be more appropriate for the thin-walled RV myocardium, have also been studied (Figure 3). Recently, an accelerated and respiratory navigator-gated look-locker imaging sequence (ANGIE) was developed for T1 quantification of the RV.<sup>33</sup> This technique provides higher spatial resolution for the thin-walled RV by using a segmented readout rather than a single-shot readout. The authors found that by using a midventricular short-axis slice during end systole at 1.5T, ANGIE provided similar RV T1 values to typical LV measurements in 9 healthy volunteers. In PH patients, ANGIE showed significantly increased RV diffuse fibrosis compared to subjects without PH, and this fibrosis was independently associated with PH even after adjustment for RV dilation and dysfunction.<sup>34</sup>

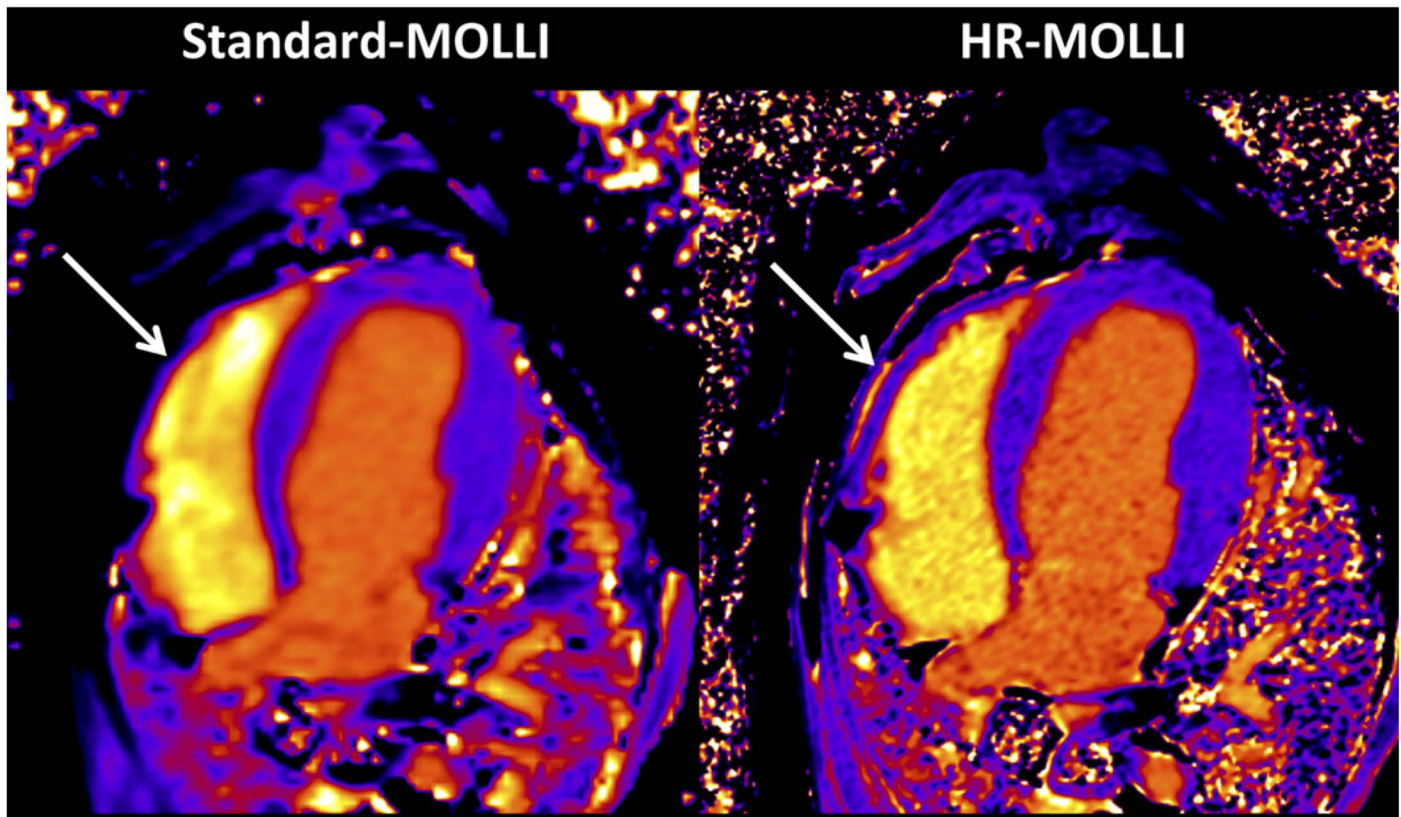


**Figure 3:** High resolution RV T1 mapping. Comparison of standard MRI technique (Standard-MOLLI) for T1 mapping to high-resolution MRI technique (HR-MOLLI) for T1 mapping. Note the better resolution of the RV free wall (white arrows). MOLLI = modified look-locker inversion recovery; RV = right ventricle.

#### PA 4D Flow Imaging

In conjunction with the development of novel MRI sequences to better understand the pathophysiology of the RV in PH, studies are also exploring additional methods such as 4D flow imaging to evaluate the pulmonary vasculature in this disease (Figure 4, see also Supplemental Clip 3). 4D flow MRI (time-resolved 3D phase-contrast MRI with 3-directional velocity encoding) offers the opportunity to noninvasively measure complex 3D hemodynamic changes with full volumetric coverage of the RV and PAs.<sup>35–37</sup> This technique provides both qualitative assessment of altered blood flow (such as helix and vortex formation) as well as quantitative hemodynamic measures such as wall shear stress, pulse wave velocity, and vorticity.

Using 4D flow MRI in the pulmonary circulation, Reiter et al. observed abnormal vortex development in the main PA in patients with both resting and exercise-induced pulmonary arterial hypertension (PAH).<sup>35</sup> Notably, the time persistence of this vortex correlated with the

degree of PH as measured by mean PA pressure. Barker et al. extended this finding by reporting a significant decrease in peak systolic velocity, peak flow, stroke volume, and wall shear stress in the main PA and both PA branches in patients with PAH compared to controls.<sup>38</sup> 4D flow imaging may also provide noninvasive assessment of more traditional hemodynamics. In PH patients with varying degrees of pulmonary vascular resistance by right heart catheterization, a multivariate regression equation that includes peak systolic vorticity, cardiac output, and relative area change in the main PA accurately estimated pulmonary vascular resistance across severe PH and normotensive populations.<sup>39</sup>

#### Exercise MRI

Recent progress in MRI-compatible exercise equipment makes it possible to evaluate the above novel sequences during stress conditions. Recreating the hemodynamic changes associated with exertion inside the MRI scanner provides unique insight into the pathophys-

ologic alterations within the RV and pulmonary vasculature that may permit earlier detection of the disease.

Several studies have focused on RV contractility during exercise and the ability of the RV to maintain an appropriate cardiac output despite increasing afterload. Using RVEF as a surrogate of RV contractile reserve, Jajjee et al. showed a decrease in RVEF with submaximal exercise in chronic PAH patients despite normal RV function at rest.<sup>40</sup> A separate study confirmed these findings and also showed that RV-PA coupling, as measured by stroke volume/end-systolic volume, was equally impaired with exercise in a small sample of patients with severe PAH.<sup>41</sup> In both studies, the key driver of poor RV contractility in patients with PAH was the inability to augment RV end-systolic volume during exercise.

In addition to standard cine images for measuring RVEF and volume, 2D-phase contrast imaging has been used to evaluate changes in PA stiffness during stress. In patients with PH, stiffness of the main PA was shown to sig-

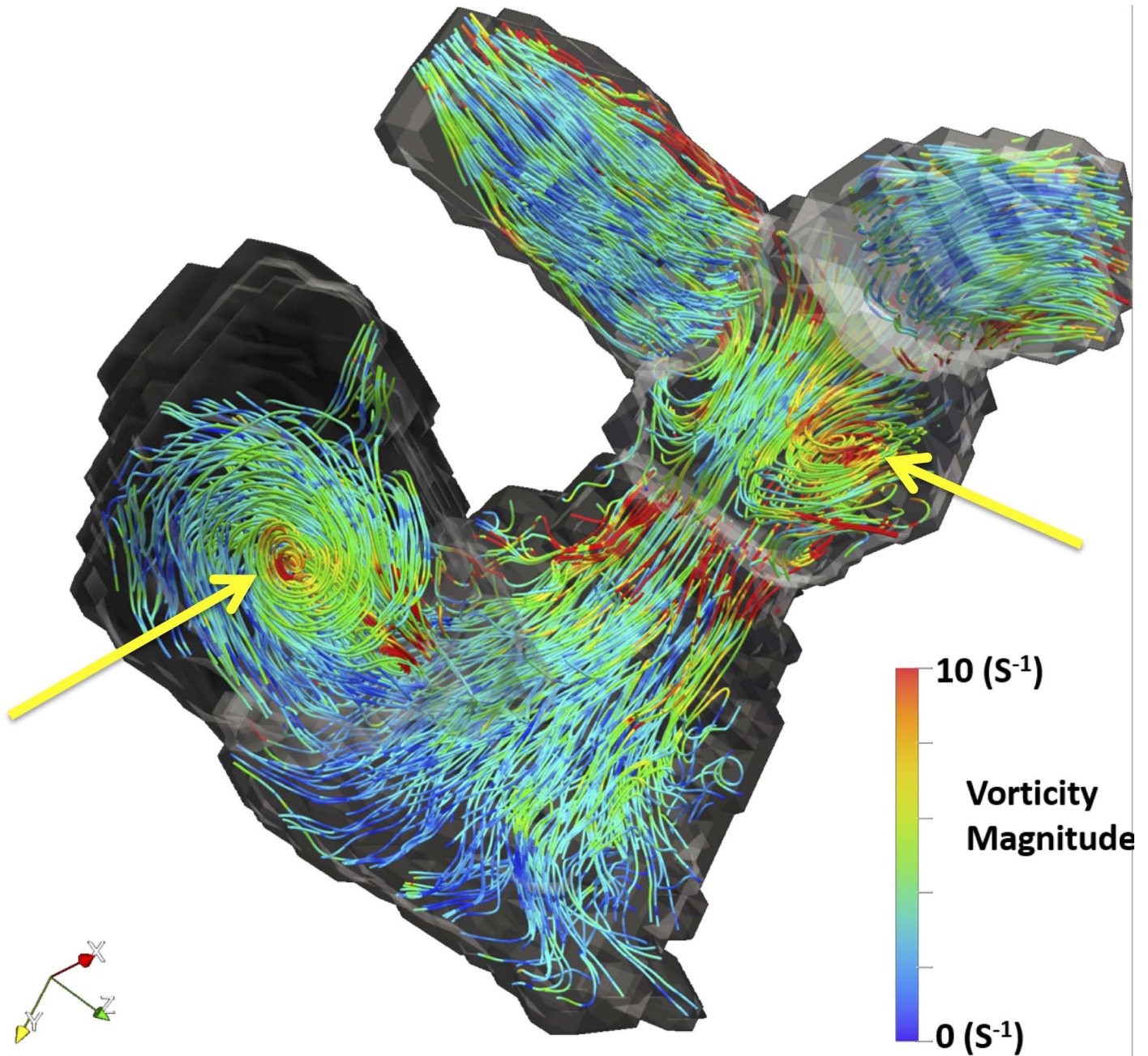


**Figure 4:** 4-dimensional flow right heart and pulmonary arteries. Altered blood flow in a patient with pulmonary hypertension as measured by vorticity. Note the vortex in the right atrium and main pulmonary artery indicating altered blood flow (yellow arrows). Image courtesy of Mohammed Elbaz, PhD.

nificantly increase during exercise when measured by pulse wave velocity.<sup>42</sup> This change significantly correlated with the stiffness index,  $\beta$ , as measured by right heart catheterization. A recent study also evaluated the value and reproducibility of feature-tracking RV strain in PAH patients during exercise MRI. Similar to previous studies showing a decline in RVEF during stress, Lin et al. showed a significant impairment in RV longitudinal strain with exercise with minimal

inter-observer variability.<sup>43</sup> Changes in RV strain during exercise might be a more sensitive marker for RV contractility than changes in RVEF.

#### *Deep Learning*

The use of artificial intelligence for cardiovascular imaging is rapidly gaining momentum. There are currently several studies evaluating deep learning approaches for assessing cardiac chamber volume, mass, and EF. These automated

methods are particularly useful for MRI where manual biventricular segmentation is time-consuming and prone to errors. One recent study highlighted the benefit of adding anatomical shape prior knowledge to a 3D neural network-based segmentation method to specifically analyze biventricular size and function in patients with PH.<sup>44</sup> These refinements to existing deep learning approaches will likely be of significant value in future PH clinical trials.

## COMPUTED TOMOGRAPHY (CT) AND POSITRON EMISSION TOMOGRAPHY (PET)

Both CT and PET play a limited but potentially useful role in the evaluation of PH. Noncontrast CT is frequently used to evaluate the lung parenchyma and is necessary to diagnose PH due to lung disease. Noncontrast CT may also provide diagnostic clues for rare types of PH such as pulmonary veno-occlusive disease or pulmonary capillary hemangiomas. Dual-energy CT is a newer method that provides both functional and anatomical data of the pulmonary vasculature. This method has been tested in patients with chronic thromboembolic PH and has performed well in generating quantitative lung perfusion and angiography using a single acquisition.<sup>45</sup>

PET provides unique metabolic information in patients with PH, but its clinical role, due in part to cost, radiation, and lack of accessibility, has yet to be established. Several studies have shown increased myocardial and lung glucose utilization in patients with PH using <sup>18</sup>F-fluorodeoxyglucose (FDG).<sup>46,47</sup> The degree of FDG uptake significantly correlates with measures of RV dysfunction. FDG uptake also appears to predict outcomes in patients with PH and may be useful in tracking therapeutic efficacy.<sup>48,49</sup>

## CONCLUSION

As therapies continue to evolve for PH, emerging noninvasive imaging techniques will be crucial for the accurate assessment of cardiac structure, function, and blood flow. Noninvasive imaging modalities also offer tremendous potential as research tools to enhance our understanding of the pathophysiology of PH. Interdisciplinary teams including cardiology, radiology, and pulmonology should jointly be involved in the selection of one or more imaging tools to best manage these patients. Future PH studies should focus on the effectiveness of applying a value-based imaging approach centered on quality, safety, and cost.

## References

1. Bossone E, D'Andrea A, D'Alto M, et al. Echocardiography in pulmonary arterial hy-

- pertension: from diagnosis to prognosis. *J Am Soc Echocardiogr.* 2013;26(1):1–14.
2. Cordina RL, Playford D, Lang I, Celermajer DS. State-of-the-art review: echocardiography in pulmonary hypertension. *Heart Lung Circ.* 2019;28(9):1351–1364.
3. Kossaify A. Echocardiographic assessment of the right ventricle, from the conventional approach to speckle tracking and three-dimensional imaging, and insights into the “right way” to explore the forgotten chamber. *Clin Med Insights Cardiol.* 2015;9:65–75.
4. Wright LM, Dwyer N, Celermajer D, Kritharides L, Marwick TH. Follow-up of pulmonary hypertension with echocardiography. *JACC Cardiovasc Imaging.* 2016;9(6):733–746.
5. Lang RM, Addetia K, Narang A, Mor-Avi V. 3-dimensional echocardiography: latest developments and future directions. *JACC Cardiovasc Imaging.* 2018;11(12):1854–1878.
6. Addetia K, Muraru D, Badano LP, Lang RM. New directions in right ventricular assessment using 3-dimensional echocardiography. *JAMA Cardiol.* 2019. doi:10.1001/jamacardio.2019.2424.
7. Leibundgut G, Rohner A, Grize L, et al. Dynamic assessment of right ventricular volumes and function by real-time three-dimensional echocardiography: a comparison study with magnetic resonance imaging in 100 adult patients. *J Am Soc Echocardiogr.* 2010;23(2):116–126.
8. Muraru D, Spadotto V, Cecchetto A, et al. New speckle-tracking algorithm for right ventricular volume analysis from three-dimensional echocardiographic data sets: validation with cardiac magnetic resonance and comparison with the previous analysis tool. *Eur Heart J Cardiovasc Imaging.* 2016;17(11):1279–1289.
9. Abouzeid CM, Shah T, Johri A, Weinsaft JW, Kim J. Multimodality imaging of the right ventricle. *Curr Treat Options Cardiovasc Med.* 2017;19(11):82.
10. Genovese D, Rashedi N, Weinert L, et al. Machine learning-based three-dimensional echocardiographic quantification of right ventricular size and function: validation against cardiac magnetic resonance. *J Am Soc Echocardiogr.* 2019;32(8):969–977.
11. Addetia K, Maffessanti F, Yamat M, et al. Three-dimensional echocardiography-based analysis of right ventricular shape in pulmonary arterial hypertension. *Eur Heart J Cardiovasc Imaging.* 2016;17(5):564–575.
12. Addetia K, Maffessanti F, Muraru D, et al. Morphologic analysis of the normal right ventricle using three-dimensional echocardiography-derived curvature indices. *J Am Soc Echocardiogr.* 2018;31(5):614–623.
13. Leary PJ, Kurtz CE, Hough CL, Waiss MP, Ralph DD, Sheehan FH. Three-dimensional analysis of right ventricular shape and function in pulmonary hypertension. *Pulm Circ.* 2012;2(1):34–40.
14. Medvedofsky D, Aronson D, Gomberg-Maitland M, et al. Tricuspid regurgitation progression and regression in pulmonary arterial hypertension: implications for right ventricular and tricuspid valve apparatus geometry and patients outcome. *Eur Heart J Cardiovasc Imaging.* 2017;18(1):86–94.
15. Narang A, Addetia K. An introduction to left ventricular strain. *Curr Opin Cardiol.* 2018;33(5):455–463.
16. Fine NM, Chen L, Bastiansen PM, et al. Outcome prediction by quantitative right ventricular function assessment in 575 subjects evaluated for pulmonary hypertension. *Circ Cardiovasc Imaging.* 2013;6(5):711–721.
17. Sachdev A, Villarraga HR, Frantz RP, et al. Right ventricular strain for prediction of survival in patients with pulmonary arterial hypertension. *Chest.* 2011;139(6):1299–1309.
18. Borges AC, Knebel F, Eddicks S, et al. Right ventricular function assessed by two-dimensional strain and tissue Doppler echocardiography in patients with pulmonary arterial hypertension and effect of vasodilator therapy. *Am J Cardiol.* 2006;98(4):530–534.
19. Kishiki K, Singh A, Narang A, et al. Impact of severe pulmonary arterial hypertension on the left heart and prognostic implications. *J Am Soc Echocardiogr.* 2019;32(9):1128–1137.
20. Freed BH, Collins JD, François CJ, et al. MR and CT imaging for the evaluation of pulmonary hypertension. *JACC Cardiovasc Imaging.* 2016;9(6):715–732.
21. Hulshof HG, Eijssvogels TMH, Kleinnibelink G, et al. Prognostic value of right ventricular longitudinal strain in patients with pulmonary hypertension: a systematic review and meta-analysis. *Eur Heart J Cardiovasc Imaging.* 2019;20(4):475–484.
22. Wright L, Dwyer N, Wahi S, Marwick TH. Relative importance of baseline and longitudinal evaluation in the follow-up of vasodilator therapy in pulmonary arterial hypertension. *JACC Cardiovasc Imaging.* 2019;12(11 Pt 1):2103–2111.
23. Shehata ML, Harouni AA, Skrok J, et al. Regional and global biventricular function in pulmonary arterial hypertension: a cardiac MR imaging study. *Radiology.* 2013;266(1):114–122.
24. de Siqueira ME, Pozo E, Fernandes VR, et al. Characterization and clinical significance of right ventricular mechanics in pulmonary hypertension evaluated with cardiovascular magnetic resonance feature tracking. *J Cardiovasc Magn Reson.* 2016;18(1):39.
25. Tello K, Dalmer A, Vanderpool R, et al. Cardiac magnetic resonance imaging-based right ventricular strain analysis for assessment of coupling and diastolic function in pulmonary hypertension. *JACC Cardiovasc Imaging.* 2019;12(11 Pt 1):2155–2164.
26. Blyth KG, Groenning BA, Martin TN, et al. Contrast enhanced-cardiovascular magnetic resonance imaging in patients with pulmonary hypertension. *Eur Heart J.* 2005;26(19):1993–1999.
27. Freed BH, Gomberg-Maitland M, Chandra S, et al. Late gadolinium enhancement cardiovas-

- cular magnetic resonance predicts clinical worsening in patients with pulmonary hypertension. *J Cardiovasc Magn Reson*. 2012;14:11.
28. Swift AJ, Rajaram S, Capener D, et al. LGE patterns in pulmonary hypertension do not impact overall mortality. *JACC Cardiovasc Imaging*. 2014;7(12):1209–1217.
  29. Reiter U, Reiter G, Kovacs G, et al. Native myocardial T1 mapping in pulmonary hypertension: correlations with cardiac function and hemodynamics. *Eur Radiol*. 2017;27(1):157–166.
  30. Saunders LC, Johns CS, Stewart NJ, et al. Diagnostic and prognostic significance of cardiovascular magnetic resonance native myocardial T1 mapping in patients with pulmonary hypertension. *J Cardiovasc Magn Reson*. 2018;20(1):78.
  31. Kawel-Boehm N, Dellas Buser T, Greiser A, Bieri O, Bremerich J, Santini F. In-vivo assessment of normal T1 values of the right-ventricular myocardium by cardiac MRI. *Int J Cardiovasc Imaging*. 2014;30(2):323–328.
  32. Tello K, Dalmer A, Axmann J, et al. Reserve of right ventricular-arterial coupling in the setting of chronic overload. *Circ Heart Fail*. 2019;12(1):e005512.
  33. Mehta BB, Chen X, Bilchick KC, Salerno M, Epstein FH. Accelerated and navigator-gated look-locker imaging for cardiac T1 estimation (ANGIE): development and application to T1 mapping of the right ventricle. *Magn Reson Med*. 2015;73(1):150–160.
  34. Mehta BB, Auger DA, Gonzalez JA, et al. Detection of elevated right ventricular extracellular volume in pulmonary hypertension using Accelerated and Navigator-Gated Look-Locker Imaging for Cardiac T1 Estimation (ANGIE) cardiovascular magnetic resonance. *J Cardiovasc Magn Reson*. 2015;17:110.
  35. Reiter G, Reiter U, Kovacs G, et al. Magnetic resonance-derived 3-dimensional blood flow patterns in the main pulmonary artery as a marker of pulmonary hypertension and a measure of elevated mean pulmonary arterial pressure. *Circ Cardiovasc Imaging*. 2008;1(1):23–30.
  36. François CJ, Srinivasan S, Schiebler ML, et al. 4D cardiovascular magnetic resonance velocity mapping of alterations of right heart flow patterns and main pulmonary artery hemodynamics in tetralogy of Fallot. *J Cardiovasc Magn Reson*. 2012;14:16.
  37. Fredriksson AG, Zajac J, Eriksson J, et al. 4-D blood flow in the human right ventricle. *Am J Physiol Heart Circ Physiol*. 2011;301(6):H2344–H2350.
  38. Barker AJ, Roldán-Alzate A, Entezari P, et al. Four-dimensional flow assessment of pulmonary artery flow and wall shear stress in adult pulmonary arterial hypertension: results from two institutions. *Magn Reson Med*. 2015;73(5):1904–1913.
  39. Kheyfets VO, Schafer M, Podgorski CA, et al. 4D magnetic resonance flow imaging for estimating pulmonary vascular resistance in pulmonary hypertension. *J Magn Reson Imaging*. 2016;44(4):914–922.
  40. Jajjee S, Quinlan M, Tokarczuk P, et al. Exercise cardiac MRI unmasks right ventricular dysfunction in acute hypoxia and chronic pulmonary arterial hypertension. *Am J Physiol Heart Circ Physiol*. 2018;315(4):H950–H957.
  41. Lin AC, Strugnell WE, Seale H, et al. Exercise cardiac MRI-derived right ventriculo-arterial coupling ratio detects early right ventricular maladaptation in PAH. *Eur Respir J*. 2016;48(6):1797–1800.
  42. Forouzan O, Dinges E, Runo JR, et al. Exercise-induced changes in pulmonary artery stiffness in pulmonary hypertension. *Front Physiol*. 2019;10:269.
  43. Lin ACW, Seale H, Hamilton-Craig C, Morris NR, Strugnell W. Quantification of biventricular strain and assessment of ventriculo-ventricular interaction in pulmonary arterial hypertension using exercise cardiac magnetic resonance imaging and myocardial feature tracking. *J Magn Reson Imaging*. 2019;49(5):1427–1436.
  44. Duan J, Bello G, Schlemper J, et al. Automatic 3D bi-ventricular segmentation of cardiac images by a shape-refined multi-task deep learning approach. *IEEE Trans Med Imaging*. 2019;38(9):2151–2164.
  45. Dournes G, Verdier D, Montaudon M, et al. Dual-energy CT perfusion and angiography in chronic thromboembolic pulmonary hypertension: diagnostic accuracy and concordance with radionuclide scintigraphy. *Eur Radiol*. 2014;24(1):42–51.
  46. Wang L, Li W, Yang Y, et al. Quantitative assessment of right ventricular glucose metabolism in idiopathic pulmonary arterial hypertension patients: a longitudinal study. *Eur Heart J Cardiovasc Imaging*. 2016;17(10):1161–1168.
  47. Saygin D, Highland KB, Farha S, et al. Metabolic and functional evaluation of the heart and lungs in pulmonary hypertension by gated 2-[18F]-Fluoro-2-deoxy-D-glucose positron emission tomography. *Pulm Circ*. 2017;7(2):428–438.
  48. Tatebe S, Fukumoto Y, Oikawa-Wakayama M, et al. Enhanced [18F]fluorodeoxyglucose accumulation in the right ventricular free wall predicts long-term prognosis of patients with pulmonary hypertension: a preliminary observational study. *Eur Heart J Cardiovasc Imaging*. 2014;15(6):666–672.
  49. Oikawa M, Kagaya Y, Otani H, et al. Increased [18F]fluorodeoxyglucose accumulation in right ventricular free wall in patients with pulmonary hypertension and the effect of epoprostenol. *J Am Coll Cardiol*. 2005;45(11):1849–1855.